

MicroRNA Profile of Tumorigenic Cells During Carcinogenesis of Lung Adenocarcinoma

Zhen-guo Zhao, Jun-yu Jin, An-mei Zhang, Lu-ping Zhang, Xin-xin Wang, Jian-guo Sun,* and Zheng-tang Chen*

Cancer Institute of PLA, Xinqiao Hospital, Third Military Medical University, Chongqing, PR China

ABSTRACT

To obtain microRNA (miRNA) profile and clarify their biological function in tumorigenic Sca-1⁺CD34⁺ cells during carcinogenesis of lung adenocarcinoma. After intranasal infection with recombinant Adeno-Cre viruses (AdV-Cre), lung adenocarcinoma was identified pathologically in *Lox-stop-lox Kras (LSL-Kras) G12D* mice. Sca-1⁺CD34⁺ cells were sorted by flow cytometry and tested for tumor-initiating ability, self-renewal and tumorigenicity. MiRNA profiles were obtained using microarray and further confirmed by real-time RT-PCR (qRT-PCR). MiRNA functions were predicted bioinformatically, and miR-294 function was verified to explore its role in tumor migration and invasion. Lung adenocarcinoma was induced in *LSL-Kras G12D* mice within 30 days. In vivo, the tumorigenicity of Sca-1⁺CD34⁺ cells was 25 times stronger than Sca-1⁻CD34⁻ cells. During tumorigenesis of lung adenocarcinoma, the expression of 145 miRNAs in Sca-1⁺CD34⁺ cells increased and 72 miRNAs decreased ($P < 0.01$). Four successively up-regulated miRNAs (miR-15a*, miR-203, miR-294 and miR-295*) and three successively down-regulated ones (miR-19b, miR-483 and miR-615-5p) were identified. Among them, miR-294 could constitutively bind to 3'-UTR of matrix metalloproteinase 3 (MMP3), and down-regulate MMP3 protein expression. MiR-294 also significantly inhibited migration and invasion of Lewis lung cancer cells. MiRNAs are characteristically expressed in tumor-initiating Sca-1⁺CD34⁺ cells of lung adenocarcinoma, and may play important roles during the carcinogenesis of lung adenocarcinoma. *J. Cell. Biochem.* 116: 458–466, 2015. © 2014 Wiley Periodicals, Inc.

KEY WORDS: LUNG ADENOCARCINOMA; TUMORIGENIC CELLS; miRNAs; CARCINOGENESIS

Lung cancer is the leading cause of cancer-related deaths worldwide. About 1,000,000 people die of lung cancer every year, including small cell lung cancer (SCLC) and non-small cell lung cancer (NSCLC) [Parkin et al., 2005]. The overall five-year survival rate for the patients with lung cancer is still below 15% [Jemal et al., 2006].

Tumorigenic cells, also designated as cancer-initiating cells or cancer stem cells (CSCs), have been proposed to be involved in cancer initiation, progression, metastasis and therapy resistance [Mimeault et al., 2007a]. Similar to normal stem cells, CSCs have unlimited capability of proliferation and self-renewal, and can generate a progeny of differentiated cells. These two kinds of cells have similar cell-surface markers, and are regulated by similar signaling pathways, including Notch, Wnt, and Hh [Tsai, 2004; Mimeault et al., 2007b]. Cumulative oncogenic mutations during carcino-

genesis may turn normal stem cells into cancer-initiating cells characterized by excessive, uncontrollable proliferation.

In recent years, the role of non-coding RNAs in lung cancer attracts much attention. MicroRNAs (miRNAs) are a class of small (19–25 nt) non-coding RNAs that regulate the expression of protein transcriptionally or post-transcriptionally [Hsu et al., 2006; Shcherbata et al., 2006]. MiRNAs exist in a wide variety of organisms, and play important roles in cell growth, apoptosis, stem cell differentiation and tumorigenesis [Cheng et al., 2005; He et al., 2005; Garzon et al., 2006]. Aberrant expression of miRNAs has been reported in many tumor types, such as lung cancer, breast cancer, and glioblastoma, indicating that miRNAs play an important part in initiation and growth of malignant tumors [Calin et al., 2004; Hayashita et al., 2005; Volinia et al., 2006]. Recent studies have revealed that miRNAs regulate differentiation of CSCs and

Zhen-guo Zhao and Jun-yu Jin contributed equally to this study.

Conflicts of interest: none.

Grant sponsor: National Science Foundation of China; Grant number: 81172070, 81071786; Grant sponsor: National High Technology R&D Program; Grant number: 2008AA02Z104.

*Correspondence to: Jian-guo Sun or Zheng-tang Chen, Cancer Institute of PLA, Xinqiao Hospital, Third Military Medical University, Chongqing 400037, PR China. E-mail: sunjg09@aliyun.com (J.S.), czt05@163.com (Z.C.)

Manuscript Received: 10 May 2014; Manuscript Accepted: 20 October 2014

Accepted manuscript online in Wiley Online Library (wileyonlinelibrary.com): 30 October 2015

DOI 10.1002/jcb.24999 • © 2014 Wiley Periodicals, Inc.

malignant transformation of normal tissue stem cells into CSCs [Ibarra et al., 2007; Yu et al., 2007].

Since first being isolated and expanded from leukemia, CSCs have been reported in several human solid tumors [Ricci-Vitiani et al., 2007]. The role of bronchioalveolar stem cells (BASCs) is striking in all the studies on lung cancer stem cells [Evans et al., 1978; Fehrenbach, 2001; Kim et al., 2005]. The regenerative potential of stem cells residing in the bronchoalveolar junction of adult lungs have been further identified and characterized. Sca-1⁺CD34⁺ cells in *Lox-stop-lox* Kras (LSL-Kras) G12D mouse model of lung carcinogenesis are capable of differentiating into type II alveolar epithelial cells and Clara cells. LSL-Kras G12D mouse is a type of transgenic animal, harboring a conditional Kras knock-in allele. Kras mutation is activated only after Cre-recombinase is delivered via recombinant adenoviral vectors [Meuwissen et al., 2001]. LSL-Kras G12D mice would develop lung adenocarcinomas after intratracheal administration of AdV-Cre. To date, the mechanism by which BASCs cumulatively mutate into lung adenocarcinoma-initiating cells remains unknown. In the current research, we planned to compare miRNA profiles between BASCs and lung adenocarcinoma stem cells, and verify miRNA function during the tumorigenesis of lung adenocarcinoma.

MATERIALS AND METHODS

CELL LINES AND ANIMALS

HEK293 and Murine Lewis lung cancer cell lines (LLC) (ATCC, Manassas, VA) were used. Recombinant Adeno-Cre viruses (AdV-Cre) were commercially purchased (Microbix Biosystems, Canada). LSL-Kras G12D mice were obtained from the MMHCC (Mouse Models Human Cancer Consortium) as a gift. BALB/c nude mice (4–5 weeks old, No. SCXK-2007001) were provided by the Experimental Animal Center of Third Military Medical University, China. All the animal experiment procedures were carried out with the approval of the Animal Ethics Committee of Third Military Medical University. Conditioned DMEM-F12 medium consisting of ITS (1:100), 20 ng/ml epidermal growth factor (EGF), 10 ng/ml basic fibroblast growth factor (bFGF), 5 mM 4-(2-hydroxyethyl)-1-piperazineethanesulfonic acid (HEPES), and 0.5% bovine serum albumin (BSA) was prepared.

CONSTRUCTION OF A MOUSE MODEL OF LUNG ADENOCARCINOMA

LSL-Kras G12D mice were used to construct the lung adenocarcinoma model. HEK293 cells and AdV-Cre were co-cultured until typical pathogenic cell infection occurred (Cytopathic Effect, CPE). Infected HEK 293 cells were digested and repeatedly frozen at -80°C and thawed at 37°C , and oscillated three times. Next, the virus supernatant was collected, purified with an Adeno - XTM Virus Purification Kit (BD Biosciences, Clontech), aliquoted, and stored at -80°C in cryopreservation media. Then a conditional knockout mouse model of lung adenocarcinoma was constructed by triggering Kras gene via intranasal infection with AdV-Cre as previously described [Meuwissen et al., 2001]. Lung tissues were taken on day 15 or day 30 and observed under a reverse microscope. Serial sections of 8–10 μm in thickness were stained with FITC-CD34, PE-Sca-1 (1: 100), and DAPI (1: 1,000).

CELL SORTING

LSL-Kras G12D mice were divided into the following groups: Group A: 0 day after intranasal infection with AdV-Cre; Group B: 15 days after intranasal infection with AdV-Cre; Group C: 30 days after intranasal infection with AdV-Cre. Lung tissues were cut into pieces and digested with 1.5 ml of dispase (0.25%), and 0.5 ml of collagenase (0.4%) for 12–16 h at 4°C , and then incubated for 60 min at 37°C . Single cell suspension was collected for cell sorting (FACS AriaTM Cell Sorter) after staining with PE-Sca-1, FITC-CD34, PE/CY7-CD31, and PE/CY5-CD45 fluorescent antibodies. CD31⁻CD45⁻Sca-1⁺CD34⁺ cells were sorted as stem cells. Among these markers, CD31⁻ and CD45⁻ were used to exclude cells from peripheral blood, and Sca-1⁺ and CD34⁺ were actual markers for stem cells from lung tissues [Kim et al., 2005]. Since Sca-1⁺ and CD34⁺ were also considered as stem cell-like markers [Batts et al., 2011; Kataoka et al., 2012], we sorted CD31⁻CD45⁻Sca-1⁻CD34⁻ cells as the control. Sca-1⁺CD34⁺ and Sca-1⁻CD34⁻ cells were designated as stem cells and control cells respectively in the following text.

COLONY-FORMING ASSAY

According to our previous research [Sun et al., 2010], colony-forming assay of Sca-1⁺CD34⁺ and Sca-1⁻CD34⁻ cells was analyzed on day 14. Sca-1⁺CD34⁺ expression was tested by immunofluorescence in the spheres with FITC-CD34 and PE-Sca-1 antibodies (1:200) for 60 min at 4°C .

CELL DIFFERENTIATION IN VITRO

Sca-1⁺CD34⁺ cells were cultured in a standard culture medium and digested with 0.25% trypsin-EDTA solution into single cells on days 2, 4, 8 and 16. After incubating PE-Sca-1 and FITC-CD34 for 30 min at 4°C , single cell suspension was fixed with 1% paraformaldehyde and analyzed by flow cytometry.

TUMORIGENICITY IN VIVO

Sca-1⁺CD34⁺ cells were subcutaneously inoculated in the right armpit of nude mice with 500K, 100K, 50K, 20K, and 10K ($1\text{K} = 1 \times 10^3$ cells), respectively ($n = 6$). Same experiments were repeated in Sca-1⁻CD34⁻ cells as a control. Tumor size was calculated by $V = LW^2/2$, in which L and W mean the long and short diameters, respectively.

MICROARRAY FABRICATION AND miRNA HYBRIDIZATION

On days 0, 15, and 30, lung tissues were taken from the LSL-Kras G12D mouse of intranasal infection with AdV-Cre (designated as groups A, B, and C above). Extraction of total RNAs and miRNA microarray hybridization were conducted as previously described [Liao et al., 2008]. Microarray (Kang Cheng Biological Chip Co. Ltd, China) was made by μ ParafloTM microfluidic chip technology, and miRNA probe sequences were obtained from the database of Sanger miRBase version 12.0 (<http://microrna.sanger.ac.uk/sequences/>). The intensity of the green signal was calculated after background subtraction and replicated spots on the same chip had been averaged by median intensity. We used Median Normalization Method to obtain "Normalized Data" (Normalized Data = [Foreground-Background]/median). The median was 50 percent quantile of miRNA

intensity, which was larger than 50 in all samples after background subtraction. Normalized data were statistically analyzed by T test ($P < 0.05$ was considered statistically significant). Each probe of mmu-miRs (miR) was repeated four times.

TARGET PREDICTION

Three online software programs, TargetScan, MiRbase, and miRanda, were used to predict miRNA targets [Liao et al., 2008; Chen et al., 2009]. Comprehensive consideration of functional conservation in different organism species, binding free energy, and scores of base matching, miR-294 and its potential target matrix metalloproteinase 3 (MMP3) were focused in the following work.

DUAL LUCIFERASE REPORTER ASSAY

Experiment design and plasmid recombination were carried out as described before [Chen et al., 2009]. Dual luciferase reporter vector pGL3-pro and control plasmid pRL-TK (Promega, USA) were used. Different 3'-UTR sequences of MMP3 were synthesized as follows. MMP3 5'→3': 5'-tctagactgtgttttaactgatgcttatagttctcatctgagctctttgtgaaaggaagtgcctttgtcatgtgctggcagaaccaaacaggagctctaga-3'; MMP3 3'→5': 5'-tctagagctcctgtttgttctgcatagcacatgctgaacaaagcactctttcacaagactcagatgaagaactataagcatcagttaaacacagctctaga-3'; and MMP3 5'→3' del without seed sequences: 5'-tctagactgtgttttaactgatgcttatagttctcatctgagctctttgtgcttatagttctcatctgagctctgttccagcagctgctatggcagaaccaaacaggagctctaga-3'. All these 3'-UTR sequences were recombined into pGL3-pro vector. Then positive clones were selected through restriction digestion by XbaI, which were confirmed by DNA sequencing. The recombinant plasmids were divided into four groups: test group (pGL3-pro-MMP3 5'→3'), control group-1 (pGL3-pro-MMP3 3'→5'), control group-2 (pGL3-pro-MMP3 5'→3' del), and empty vector group (pGL3-pro). LLC cells were transfected with recombinant plasmids via lipofectamine 2000 (Lipo 2000) (Invitrogen, USA) when cell confluence reached 60–80% in a 24 well plate. Cotransfection reaction contained 200 ng of pGL3-vector, 200 ng of pRL-TK vector and 2.5 μl of miR-294 mimics. LLC cells were collected after 24 h of incubation and analyzed for luciferase activity. The change of luciferase ratio of Firefly/Renilla represented the interaction between miR-294 and 3'-UTR of MMP3.

REAL-TIME RT-PCR (qRT-PCR)

We followed the previous protocol for primer design and SYBR Green qPCR of miRNAs [Chen et al., 2005; Liao et al., 2008]. The up-stream and down-stream primers of miRNAs and internal control U6 RNA were as follows. U6: 5'-gcttcggcagcacatataactaaat-3', 5'-cgcttcacgaattgtcg-tgtcat-3'; miR-15a*: 5'-accaggccatactgtgct-3', 5'-tgctgtcgtgaggagtc-3'; miR-295*: 5'-gactcaaatgtggggca-3', 5'-cagtgcgtgctgagtc-3'; miR-294: 5'-ggcaaatgtctccctt-3', 5'-cagtgcgtgctgaggagtc-3'; miR-203: 5'-ggggtgaaatgttttagga-3', 5'-tgctgtcgtgaggagtc-3'; miR-19b: 5'-acctg-tgcaaatcatg-3', 5'-tgctgtcgtgaggagtc-3'; miR-483: 5'-ggaagacgggagaa-gaga-3', 5'-cagtgcgtgctgaggagtc-3'; miR-615-5p: 5'-agggggtcccccgtg-3', 5'-gtcgtgctgaggagtc-3'. As for qRT-PCR of target gene MMP3, the up-stream and down-stream primers of MMP-3 and internal control β-actin were as follows. MMP3: 5'-cacatcacctacaggattgtga-atta-3', 5'-catgagccaagactgttcca-3'; β-actin: 5'-tcaagatcattgctcctcct-gag-3', 5'-acatctgctggaaggtggaca-3'.

WESTERN BLOT

Procedures of Western blot were described in detail in our previous work [Ma et al., 2011]. Simply, miR-294 mimics and miR negative control (RiboBio Co. Ltd., Guangzhou, China) were transfected into LLC by lipofectamine 2000, respectively, to reach a final concentration of 30 nM. After 48 h, MMP-3 mRNA and protein were detected by qRT-PCR and Western blot, respectively. MMP3 primary antibody (Abcam, USA) and secondary antibody labeled with horseradish peroxidase (HRP) (Zhongshan Biotechnology Company, Beijing, China) were used in Western blot.

MATRIGEL INVASION AND TRANSWELL MIGRATION ASSAYS

MiR-294 mimics and miR negative control were transfected into LLC as described above. Matrigel invasion and transwell migration assays were performed according to a earlier report [Batts et al., 2011]. Each experiment was repeated three times.

RESULTS

CONSTRUCTION OF MOUSE MODEL OF LUNG ADENOCARCINOMA

To confirm successful Lox-stop-lox modification of experimental mice, we designed primers to amplify LSL-Kras fragment from genomic DNA by PCR. The primer sequences were as follows. 5'-cctttacaagcgcagcagactgtaga-3', 5'-agctagccaccatggcttgtagtaagctt-gca-3'. A 550-bp PCR product was obtained, preliminarily proving that the mouse model was LSL-Kras G12D (Fig. 1a). Immunofluorescence showed that green fluorescent FITC-CD34 was distributed at the joint of the alveolar isolation (Fig. 1b), and red fluorescent PE-Sca-1 at terminal and respiratory bronchioles, localized in the cytoplasm around the nucleus (Fig. 1c). DAPI labeled cell nuclei were prominently blue (Fig. 1d), and a few Sca-1⁺CD34⁺ cells with yellow fluorescence in large and round shape were distributed at BADJ between alveolar duct and respiratory bronchioles (Fig. 1e).

In Group A, the lung tissues were pink and smooth, without any abnormal change such as nodules or hyperemia (Fig. 1f), and no dysplasia appeared in pulmonary bronchial epithelium in HE staining (Fig. 1h). In Group B, atypical hyperplasia of pulmonary bronchial epithelium appeared in bronchioles and the mucosa became thicker (Fig. 1i). In Group C, dim gray nodules appeared on the surface (Fig. 1g), and pulmonary bronchial epithelium showed diffused adenocarcinoma nests (Fig. 1j).

ISOLATION AND CULTURE OF Sca-1⁺CD34⁺ CELLS

The expression of Sca-1 and CD34 in lung tissues was analyzed by flow cytometry. We observed 0.7–1.1% Sca-1⁺CD34⁺ cells and 1.7–2.0% Sca-1⁻CD34⁻ cells, and sorted the cells using flow cytometry. This subpopulation was highly purified (71.5–80%). At the original position where the positive cells existed, only a few cells left.

IDENTIFICATION OF TUMORIGENIC STEMNESS OF Sca-1⁺CD34⁺ CELLS

Sorted Sca-1⁺CD34⁺ cells (1.5×10^5) were cultured in a 12-well plate with conditioned culture medium. On day 3, three to five epithelioid colonies appeared. On day 10, most of the colonies turned into globular spheres composed of more than 50 cells (Fig. 2a). In the

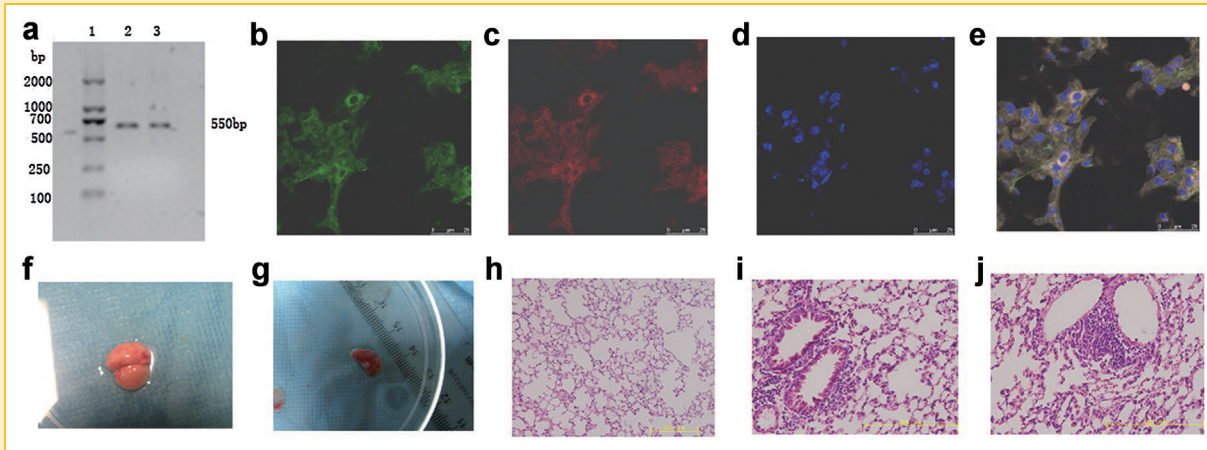


Fig. 1. Induced lung adenocarcinoma by recombinant Adeno-Cre virus (AdV-Cre) in Lox-stop-lox Kras (LSL-Kras) G12D mice. PCR product of 550bp LSL-Kras fragment in conditional knockout mice (Lane 1: DNA marker; lane 2 and 3: PCR product of LSL-Kras fragment) (a). Immunofluorescence staining of Sca-1⁺CD34⁺ cells in the same slides of lung tissues. CD34-FITC (b), Sca-1-PE (c), DAPI staining of cell nuclei (d) and merging of b and c (e). In Group A (day 0), lung tissues displayed smooth surface (f, h). In Group B (day 15), pulmonary bronchial epithelium atypical hyperplasia appeared in bronchioles and the mucosa became thicker (i). In Group C (day 30), dim gray nodules appeared on the lung surface (g), and atypical hyperplasia appeared on the bronchial epithelium covered by adenocarcinoma nests (j).

standard culture medium, Sca-1⁺CD34⁺ cells displayed semi-adherent growth, oval or spindle cell morphology (Fig. 2b).

FITC-CD34 and PE-Sca-1 immunocytochemical staining was done in spheres on day 6. In the merged picture, double-stained cells with both FITC and PE fluorescence were distributed in the

cytoplasm around the nucleus, indicating that both CD34 and Sca-1 were highly expressed in spheres (Fig. 2c-f).

In colony formation assay, Sca-1⁺CD34⁺ cells could produce significantly more colonies or spheres than Sca-1⁻CD34⁻ cells in both standard culture medium and conditioned culture medium

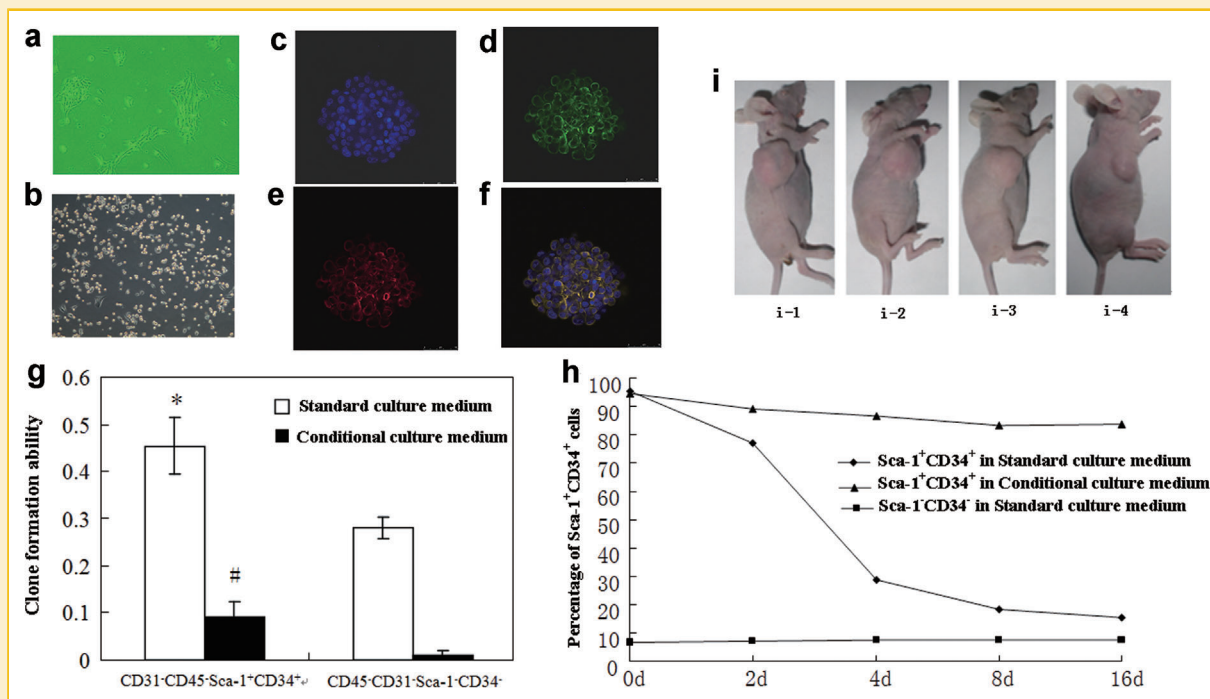


Fig. 2. Tumorigenicity of Sca-1⁺CD34⁺ cells from induced lung adenocarcinoma. In conditioned culture medium, Sca-1⁺CD34⁺ cells showed typical "clone growth" (a). In standard culture medium, Sca-1⁺CD34⁺ cells were in semi-adherent growth (b). The cells were labeled with DAPI (c), FITC-CD34 (d), and PE-Sca-1 (e). Yellow fluorescent spheres labeled by CD34, Sca-1 double positive cells (f). Sca-1⁺CD34⁺ cells could form more clones than Sca-1⁻CD34⁻ cells (g) in standard culture medium (**P* < 0.01) and conditioned culture medium (#*P* < 0.01). The sphere formation ability of Sca-1⁺CD34⁺ and Sca-1⁻CD34⁻ in standard culture medium (**P* < 0.01) or conditioned culture medium (h). Tumor generating experiment (i), i-1 and i-2 for Sca-1⁺CD34⁺ cells, i-3 for non-sorting cells of lung tissues and i-4 for Sca-1⁻CD34⁻ cells.

($P < 0.01$). The colony formation ratios in Sca-1⁺CD34⁺ and Sca-1⁻CD34⁻ cells were 10% and 1%, respectively (Fig. 2g).

When being transferred into a standard culture medium with 10% FBS, Sca-1⁺CD34⁺ cell spheres adhered to the culture plate in 12 h. The percentage of Sca-1⁺CD34⁺ declined with the culture time. After 16 days, Sca-1⁺CD34⁺ percentage decreased to a normal level of parental LLC cells, indicating that Sca-1⁺CD34⁺ could differentiate into other molecular phenotypes of cells (Fig. 2h).

In xenograft experiment in nude mice, tumors could be observed in every group when 500 K cells were inoculated subcutaneously. Sca-1⁺CD34⁺ cells gave rise to larger tumors than the control ($P < 0.01$, Table I). In gradient assay, Sca-1⁺CD34⁺ cells could generate tumors when 10 K cells were inoculated, while Sca-1⁻CD34⁻ cells could not grow into a tumor when 50 K cells were inoculated. To reach a similar tumorigenic efficacy, the quantity of required Sca-1⁺CD34⁺ cells was 20 K while that of Sca-1⁻CD34⁻ cells 500 K. Thus, the tumorigenicity of Sca-1⁺CD34⁺ cells was 25 times stronger than Sca-1⁻CD34⁻ cells (Fig. 2i, Table 1).

miRNA PROFILE OF Sca-1⁺CD34⁺ CELLS

MiRNA microarray fluorescent signals in groups A, B and C are shown in Fig. 3a, b, and c. MiRNAs were regarded as measurable transcription elements if they satisfied two conditions: signal intensity $> 3 \times$ background standard deviation and spot coefficient of variability (spot CV) < 0.5 . The clustering and correlation coefficient matrix was performed and mmu-miRNA profiles were obtained. As mentioned above, experimental LSL-Kras G12D mice were divided into 3 groups (groups A, B and C) according to days 0, 15 and 30 after intranasal infection with AdV-Cre. Although the lung tissues from groups A, B and C were of very similar origin, differences in miRNA profile were detectable. A total of 145 miRNAs increased successively in groups A, B, and C ($P < 0.01$); 72 miRNAs decreased successively ($P < 0.01$) (Supplemental Table. S1 & S2); four miRNAs (miR-15a*, miR-203, miR-294 and miR-295*) increased successively over 1.2 fold in groups A, B, and C; three miRNAs (miR-19b, miR-483 and miR-615-5p) decreased successively over 0.5-fold. Quantitative analysis of microarrays in group B/A and group C/B showed significant difference ($P < 0.05$, Table II). All the data had been uploaded and submitted onto Gene Expression Omnibus (GEO) database (<http://www.ncbi.nlm.nih.gov/geo/query/acc.cgi?acc=GSE60001>).

Special attention was paid to the successively increased or decreased miRNAs between groups A, B and C. To verify the accuracy of the miRNA array, seven miRNAs were chosen for further qRT-PCR assay. Amplification curve of miR-294 was demonstrated as a representative of qRT-PCR assay (Fig. 3d). The results of qRT-PCR

assay were basically consistent with microarray, thus validating the authenticity of miRNA microarray (Fig. 3e-f). Quantitative analysis of qRT-PCR assay in group B/A and group C/B also showed significant difference ($P < 0.05$, Table 2).

TARGET VERIFICATION

According to bioinformatics analysis, most of the targets were oncogenes, anti-oncogenes or regulatory factors involved in metabolism, cell cycle, transcription, apoptosis, proliferation, and differentiation (Supplemental Table S3). For example, dozens of potential genes were targeted by miR-294, such as Wee1, Gpr34, MMP3, Cdca4, Hsp110, Atp10d, Egr3, and Map3k1. Several potential targets were chosen to verify (data not shown). Here MMP3 was shown as a target gene.

In dual luciferase reporter assay, 48 h after cotransfection of recombinant plasmids and miR-294 mimics into LLC cells, luciferase activities of firefly and Renilla were detected in all the four groups. Firefly/Renilla ratios were 6.43 ± 1.03 , 13.75 ± 2.61 , 13.59 ± 1.67 , and 11.90 ± 1.49 in test group, control group-1, control group-2 and empty vector group, respectively. A significant decrease was observed in the test group instead of the other three groups ($P < 0.05$).

In qRT-PCR assay, miR-294 expression in LLC cells with miR-294 mimics transfection was 2.86 and 7.37 folds higher than that in miR negative control transfection and parental LLC cells, respectively. Then MMP3 mRNA was also detected by qRT-PCR. No significant changes were found in different transfection assays (Fig. 4a). However, in Western blot, miR-294 mimics could significantly decrease MMP3 protein expression compared with miR negative control transfection and parental LLC cells ($P < 0.05$) (Fig. 4b).

FUNCTIONAL ANALYSIS OF miR-294

In matrigel invasion assay, the invading tumor cells were 108.33, 165.00 and 168.67 on average in miR-294 mimics transfection, miR negative control transfection and parental LLC cells, respectively. The results showed that miR-294 mimics (Fig. 4c) significantly decreased invasion of LLC cells compared with miR negative control (Fig. 4d) and parental LLC cells (Fig. 4e, $P < 0.05$).

In transwell migration assay, similar results were observed. The migrating tumor cells were 109.00, 177.33 and 190.33 on average in miRNA mimics transfection, miR negative control transfection and parental LLC cells, respectively. MiR-294 mimics (Fig. 4f) significantly decreased migration of LLC cells compared with miR negative control (Fig. 4g) and parental LLC cells (Fig. 4h, $P < 0.05$).

TABLE I. Tumor Growth After Gradient Density Explantation

Cells	Tumor growth					Tumor weight(g)	Tumor volume(mm ³)
	500K	100K	50K	20K	10K	500K	500K
Sca-1 ⁺ CD34 ⁺	6/6	6/6	6/6	5/6	1/6	$5.35 \pm 0.26^*$	$7880.50 \pm 264.93^*$
Sca-1 ⁻ CD34 ⁻	5/6	2/6	0/6	0/6	0/6	2.29 ± 0.25	1422.02 ± 87.68

* $P < 0.01$, vs Sca-1⁻CD34⁻

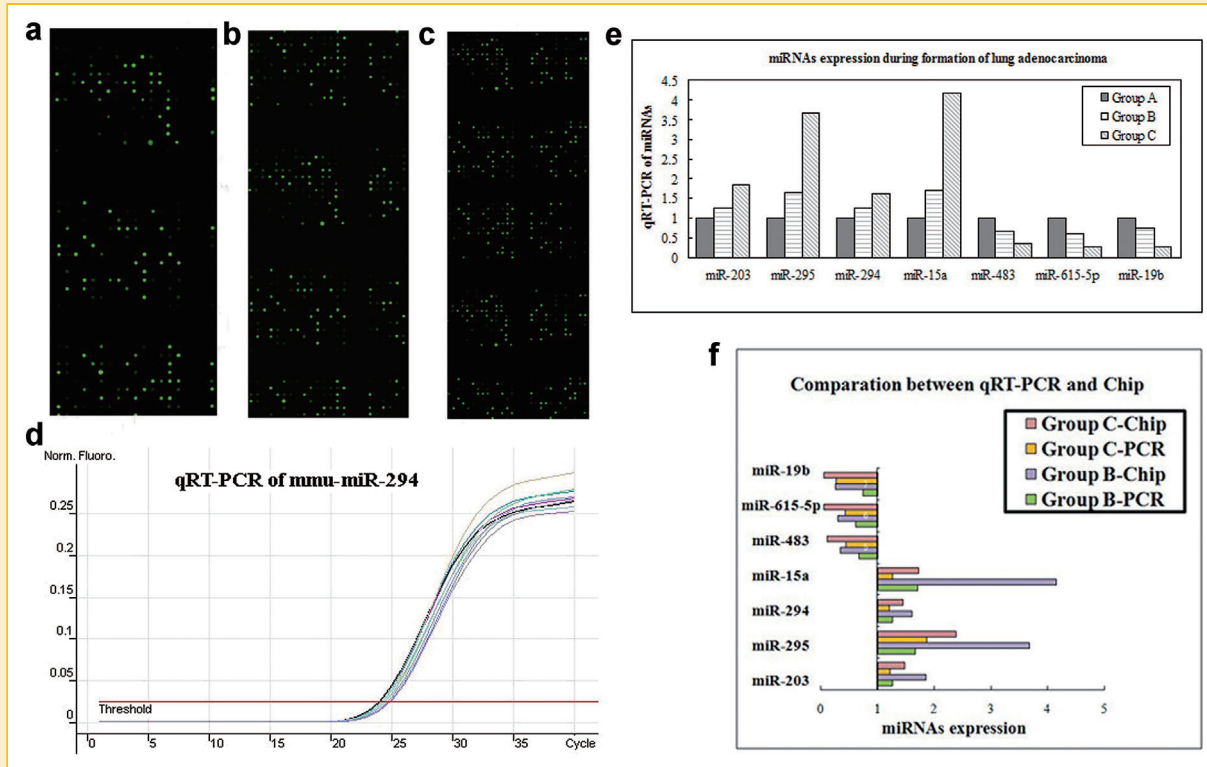


Fig. 3. miRNA profile of Sca-1⁺CD34⁺ cells and associated miRNAs in tumorigenesis. Fluorescent signals of miRNA microarray are shown of Sca-1⁺CD34⁺ cells from mice with intranasal infection of AdV-Cre at day 0 (a, Group A), day 15 (b, Group B) and day 30 (c, group C). qRT-PCR amplification curve of mmu-miR-294 was exhibited as a representative (d). Seven miRNAs detected by qRT-PCR in different groups (e) and compared with miRNA chips (f).

DISCUSSION

It is well known that TICs are the source of non-stem cancer cells and the root of treatment resistance of cancer. A previous study has shown that stem-like cancer cells derived from normal cell transition displays tumorigenicity (Chambers and Smith, 2004). In the present study, we not only developed a mouse model of lung adenocarcinoma, but also clarified the molecular changes and biological mechanism underlying lung carcinogenesis. We found that Sca-1⁺CD34⁺ cells showed strong colony-forming and proliferation

capabilities in vitro and they could differentiate into Sca-1⁻CD34⁻ cells in the serum. By detecting tumorigenicity, we found that Sca-1⁺CD34⁺ cells displayed tumorigenic efficacy 25 times higher than Sca-1⁻CD34⁻ cells. These findings were consistent with earlier research [Kim et al., 2005] and paved the way for further work.

It is believed that miRNAs take part in the tumorigenesis of many solid cancers such as breast cancer [Volinia et al., 2006; Yu et al., 2007]. Several studies have also shown that aberrant expression of miRNAs is involved in generation of lung cancer, such as miR-17-92, miR-21, miR-17-5p, miR-191, miR-128b, miR-199a-1, miR-155,

TABLE II. miRNAs Increased/Decreased Successively in A, B and C Groups

miRNAs	miRNA microarray ^a			qRT-PCR (miRNA/U6) ^a			
	A	B	C	B/A	C/B	B/A	C/B
miR-203	0.330 ± 0.036	0.402 ± 0.040	0.490 ± 0.025	1.218	1.220	1.26	1.47
miR-295*	0.002 ± 0.003	0.004 ± 0.001	0.005 ± 0.004	1.874	1.270	1.66	2.22
miR-294	0.171 ± 0.018	0.206 ± 0.011	0.249 ± 0.010	1.202	1.211	1.26	1.28
miR-15a*	0.037 ± 0.003	0.047 ± 0.005	0.065 ± 0.007	1.268	1.362	1.71	2.43
miR-483	0.046 ± 0.001	0.021 ± 0.003	0.005 ± 0.001	0.446	0.254	0.67	0.52
miR-615-5p	0.029 ± 0.012	0.012 ± 0.003	0.002 ± 0.002	0.433	0.141	0.62	0.48
miR-19b	0.031 ± 0.006	0.008 ± 0.004	0.002 ± 0.001	0.268	0.212	0.75	0.35

^aSignificant difference in Group B/A and Group C/B, respectively ($P < 0.05$).

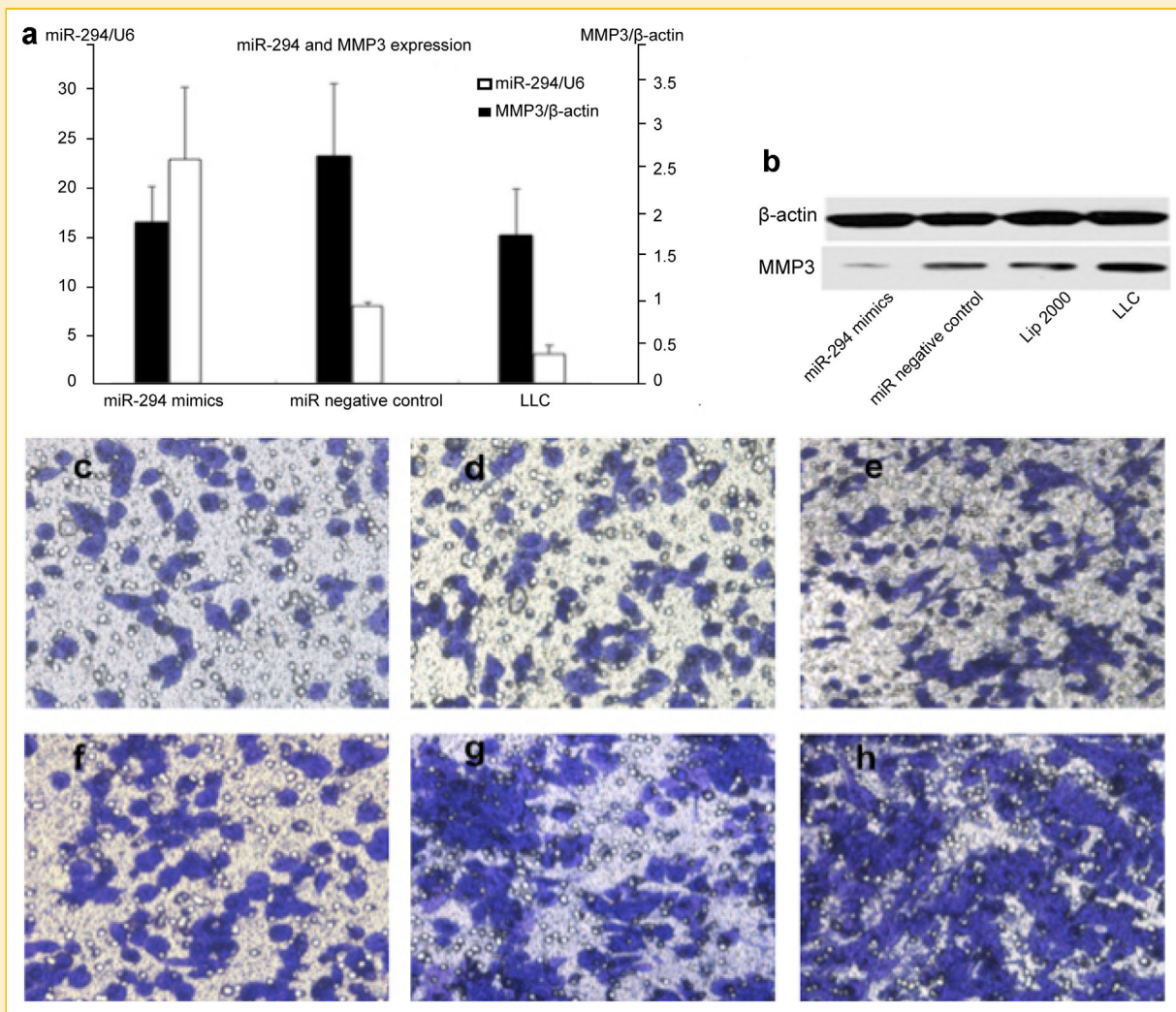


Fig. 4. Target verification and biological function of miR-294 in LLC cells. miR-294 (a), MMP3 mRNA (a) and MMP3 protein (b) detected in LLC cells after miR-294 mimics transfection, miR negative control transfection and parental LLC cells by qRT-PCR and Western blot, respectively. In matrigel invasion assay (Crystal Violet Staining, 200 \times), miR-294 mimics (c) decreased invasion cell numbers compared with miR negative control (d) and parental LLC cells (e). In transwell migration assay (Crystal Violet Staining, 200 \times), mmu-miR-294 mimics (f) decreased migration cell numbers compared with miR negative control (g) and parental LLC cells (h).

and let-7 [Hayashita et al., 2005; Volinia et al., 2006]. We previously identified fifty miRNAs in TICs from human A549 lung cancer cells [Lin et al., 2012]. Recently, it was reported that five miRNAs (let-7a, miR-221, miR-137, miR-372, and miR-182*) are closely related to the survival and tumor relapse in NSCLC patients [Yu et al., 2008]. Nevertheless, little is known about miRNA function in lung carcinogenesis. By isolating Sca-1⁺CD34⁺ cells from lung tissues, we investigated the changes in miRNA profiles in carcinogenesis of lung adenocarcinoma. Our research indicates that several miRNAs, successively over-expressed or under-expressed in Sca-1⁺CD34⁺ tumorigenic cells, probably play important roles in lung adenocarcinoma initiation.

We further explored down-stream target genes of the miRNAs of interest. We predicted and verified that miR-294 down-regulated MMP3 target gene. Matrix metalloproteinases (MMPs) are a family of proteolytic enzymes that degrade the extracellular matrix and play important roles in tumor invasion and metastasis [Hewitt et al., 1991;

Chambers and Matrisian, 1997]. MMP3, a member of MMPs, has a function analogous to its homologue MMP9 that can promote cancer cell invasion, migration and metastasis in several tumors including lung cancer [Fang et al., 2005; Zhang et al., 2011]. Our study revealed that miR-294 constitutively binds to 3'-UTR of MMP3. Subsequent research showed that miR-294 mimics can decrease MMP3 protein expression, though no obvious change in mRNA level was observed. Matrigel invasion assay and transwell migration assay further confirmed the inhibition of the migration and invasion in LLC cells by miR-294 mimics transfection.

MiR-294 has been reported to promote the induction of pluripotency in embryonic stem cell (ESC) [Judson et al., 2009; Hanina et al., 2010]. Its expression increases during G1 phase of ESC cycle [Hanina et al., 2010; Wang et al., 2013]. Consistent with these findings, we observed that miR-294 is highly expressed in stem cell-like Sca-1⁺CD34⁺ cells, suggesting that miR-294 up-regulation correlates with stemness. Of interest, we found that miR-294 mimics

could decrease MMP3 protein expression and suppress LLC cell invasion and migration. To our best knowledge, this is the first time, miR-294 function was tested in regulating MMP3 and cancer cell invasion and migration. miR-294 probably plays different roles in different tumor types and different pathological processes. Since MMP3 is critical for the maintenance of stemness for CSCs that exhibit potent capacities of invasion and metastasis [Jin et al., 2013], the up-regulation of miR-294 in CSCs and its regulation on MMP3 in LLC suggested a novel cell-type dependent feedback regulatory mechanism, by which miR-294 may negatively modulate the stemness. Our subsequent work will focus on the biological function of miR-294 in regulating self-renewal and metastasis in stem cell-like cancer cells.

In this study, miR-294 has been used to demonstrate the biological function of miRNAs in Sca-1⁺CD34⁺ tumorigenic cells. The findings are consistent with our hypothesis that miRNAs play important roles in malignant transformation of BASCs. We will further investigate biological functions of more miRNAs and their targets in the future.

CONCLUSIONS

Here, we investigated the miRNA profile of the Sca-1⁺CD34⁺ population in an LSL-Kras G12D mouse model of lung adenocarcinoma. miR-294 could down-regulate MMP3 and significantly inhibit migration and invasion of LLC cells. Our identification of Sca-1⁺CD34⁺-related miRNAs can be a start to exploring the functions of these miRNAs. This study adds a new dimension to our understanding of the carcinogenesis of lung adenocarcinoma and assists oncologic biologists and clinical oncologists in designing novel therapeutic strategies.

ACKNOWLEDGEMENTS

We give special thanks to Prof. Rongxia Liao (Medical English Department, Third Military Medical University) for English editing.

REFERENCES

Batts TD, Machado HL, Zhang Y, Creighton CJ, Li Y, Rosen JM. 2011. Stem cell antigen-1 (sca-1) regulates mammary tumor development and cell migration. *PLoS ONE* 6:e27841.

Calin GA, Sevignani C, Dumitru CD, Hyslop T, Noch E, Yendamuri S, Shimizu M, Rattan S, Bullrich F, Negrini M, Croce CM. 2004. Human microRNA genes are frequently located at fragile sites and genomic regions involved in cancers. *Proc Natl Acad Sci USA* 101:2999–3004.

Chambers AF, Matrisian LM. 1997. Changing views of the role of matrix metalloproteinases in metastasis. *J Natl Cancer Inst* 89:1260–1270.

Chambers I, Smith A. 2004. Self-renewal of teratocarcinoma and embryonic stem cells. *Oncogene* 23:7150–7160.

Chen C, Ridzon DA, Broomer AJ, Zhou Z, Lee DH, Nguyen TJ, Barbisin M, Xu NL, Mahuvakar VR, Andersen MR, Lao KQ, Livak KJ, Guegler KJ. 2005. Real-time quantification of microRNAs by stem-loop RT-PCR. *Nucleic Acids Res* 33:e179.

Chen H, Sun JG, Cao XW, Ma XG, Xu JP, Luo FK, Chen ZT. 2009. Preliminary validation of ERBB2 expression regulated by miR-548d-3p and miR-559. *Biochem Biophys Res Commun* 385:596–600.

Cheng AM, Byrom MW, Shelton J, Ford LP. 2005. Antisense inhibition of human miRNAs and indications for an involvement of miRNA in cell growth and apoptosis. *Nucleic Acids Res* 33:1290–1297.

Evans MJ, Cabral-Anderson LJ, Freeman G. 1978. Role of the Clara cell in renewal of the bronchiolar epithelium. *Lab Invest* 38:648–653.

Fang S, Jin X, Wang R, Li Y, Guo W, Wang N, Wang Y, Wen D, Wei L, Zhang J. 2005. Polymorphisms in the MMP1 and MMP3 promoter and non-small cell lung carcinoma in North China. *Carcinogenesis* 26:481–486.

Fehrenbach H. 2001. Alveolar epithelial type II cell: Defender of the alveolus revisited. *Respir Res* 2:33–46.

Garzon R, Fabbri M, Cimmino A, Calin GA, Croce CM. 2006. MicroRNA expression and function in cancer. *Trends Mol Med* 12:580–587.

Hanina SA, Mifsud W, Down TA, Hayashi K, O'Carroll D, Lao K, Miska EA, Surani MA. 2010. Genome-wide identification of targets and function of individual MicroRNAs in mouse embryonic stem cells. *PLoS Genet* 6:e1001163.

Hayashita Y, Osada H, Tatematsu Y, Yamada H, Yanagisawa K, Tomida S, Yatabe Y, Kawahara K, Sekido Y, Takahashi T. 2005. A polycistronic microRNA cluster, miR-17–92, is overexpressed in human lung cancers and enhances cell proliferation. *Cancer Res* 65:9628–9632.

He L, Thomson JM, Hemann MT, Hernando-Monge E, Mu D, Goodson S, Powers S, Cordon-Cardo C, Lowe SW, Hannon GJ, Hammond SM. 2005. A microRNA polycistron as a potential human oncogene. *Nature* 435:828–833.

Hewitt RE, Leach IH, Powe DG, Clark IM, Cawston TE, Turner DR. 1991. Distribution of collagenase and tissue inhibitor of metalloproteinases (TIMP) in colorectal tumours. *Int J Cancer* 49:666–672.

Jin X, Jin X, Sohn YW, Yin J, Kim SH, Joshi K, Nam DH, Nakano I, Kim H. 2013. Blockade of EGFR signaling promotes glioma stem-like cell invasiveness by abolishing ID3-mediated inhibition of p27(KIP1) and MMP3 expression. *Cancer Lett* 328:235–242.

Hsu PW, Huang HD, Hsu SD, Lin LZ, Tson AP, Tsenq CP, Stadler PF, Washietl S, Hofacker IL. 2006. MiRNome: genomic maps of microRNA genes and their target genes in mammalian genomes. *Nucleic Acids Res* D135–D139.

Ibarra I, Erlich Y, Muthuswamy SK, Sachidanandam R, Hannon GJ. 2007. A role for microRNAs in maintenance of mouse mammary epithelial progenitor cells. *Genes Dev* 21:3238–3243.

Jemal A, Siegel R, Ward E, Murray T, Xu J, Smigal C, Thun MJ. 2006. Cancer statistics, 2006. *CA Cancer J Clin* 56:106–130.

Judson RL, Babiarz JE, Venere M, Brelloch R. 2009. Embryonic stem cell-specific microRNAs promote induced pluripotency. *Nat Biotechnol* 27:459–461.

Kataoka H, Okabe H, Amano S, Yamada E, Ishida M, Kushima R, Kobayashi TK. 2012. Cytologic and immunophenotypic features of CD34⁺ stem cells in body cavity fluids. *Acta Cytol* 56:401–407.

Kim CF, Jackson EL, Woolfenden AE, Lawrence S, Babar I, Voqel S, Crowley D, Brownson RT, Jacks T. 2005. Identification of bronchioalveolar stem cells in normal lung and lung cancer. *Cell* 121:823–835.

Liao R, Sun J, Zhang L, Lou G, Chen M, Zhou D, Chen Z, Zhang S. 2008. MicroRNAs play a role in the development of human hematopoietic stem cells. *J Cell Biochem* 104:805–817.

Lin S, Sun JG, Wu JB, Long HX, Zhu CH, Xiang T, Ma H, Zhao ZQ, Yao Q, Zhang AM, Zhu B, Chen ZT. 2012. Aberrant microRNAs expression in CD133⁺/CD326⁺ human lung adenocarcinoma initiating cells from A549. *Mol Cells* 33:277–283.

Ma H, Yao Q, Zhang AM, Lin S, Wang XX, Wu L, Sun JG, Chen ZT. 2011. The effects of artesunate on the expression of EGFR and ABCG2 in A549 human lung cancer cells and a xenograft model. *Molecules* 16:10556–10569.

Meuwissen R, Linn SC, van der Valk M, Mooi WJ, Berns A. 2001. Mouse model for lung tumorigenesis through Cre/lox controlled sporadic activation of the K-Ras oncogene. *Oncogene* 20:6551–6558.

Mimeault M, Hauke R, Batra SK. 2007a. Stem cells: A revolution in therapeutics-recent advances in stem cell biology and their therapeutic applications in regenerative medicine and cancer therapies. *Clin Pharmacol Ther* 82:252–264.

Mimeault M, Hauke R, Mehta PP, Batra SK. 2007b. Recent advances in cancer stem/progenitor cell research; therapeutic implications for overcoming resistance to the most aggressive cancers. *J Cell Mol Med* 11:981–1011.

Parkin DM, Bray F, Ferlay J, Pisani P. 2005. Global cancer statistics, 2002. *CA Cancer J Clin* 55:74–108.

Ricci-Vitiani L, Lombardi DG, Pilozzi E, Biffoni M, Todaro M, Peschle C, De Maria R. 2007. Identification and expansion of human colon-cancer-initiating cells. *Nature* 445:111–115.

Shcherbata HR, Hatfield S, Ward EJ, Reynolds S, Fischer KA, Ruohola-Baker H. 2006. The MicroRNA pathway plays a regulatory role in stem cell division. *Cell Cycle* 5:172–175.

Sun JG, Liao RX, Qiu J, Jin JY, Wang XX, Duan YZ, Chen FL, Hao P, Xie QC, Wang ZX, Li DZ, Chen ZT, Zhang SX. 2010. Microarray-based analysis of microRNA expression in breast cancer stem cells. *J Exp Clin Cancer Res* 29:174.

Tsai RY. 2004. A molecular view of stem cell and cancer cell self-renewal. *Int J Biochem Cell Biol* 36:684–694.

Volinia S, Calin GA, Liu CG, Ambs S, Cimmino A, Petrocca F, Visone R, Iorio M, Roldo C, Ferracin M, Prueitt RL, Yanaihara N, Lanza G, Scarpa A, Vecchione A, Negrini M, Harris CC, Croce CM. 2006. A microRNA expression

signature of human solid tumors defines cancer gene targets. *Proc Natl Acad Sci USA* 103:2257–2261.

Wang Y, Melton C, Li YP, Shenoy A, Zhang XX, Subramanyam D, Blelloch R. 2013. MiR-294/miR-302 promotes proliferation, suppresses G1-S restriction point, and inhibits ESC differentiation through separable mechanisms. *Cell Rep* 4:99–109.

Yu SL, Chen HY, Chang GC, Chen CY, Chen HW, Singh S, Cheng CL, Yu CJ, Lee YC, Chen HS, Su TJ, Chiang CC, Li HN, Hong QS, Su HY, Chen CC, Chen WJ, Liu CC, Chan WK, Chen WJ, Li KC, Chen JJ, Yang PC. 2008. MicroRNA signature predicts survival and relapse in lung cancer. *Cancer Cell* 13:48–57.

Yu F, Yao H, Zhu P, Zhang X, Pan Q, Gong C, Huang Y, Hu X, Su F, Lieberman J, Song E. 2007. Let-7 regulates self renewal and tumorigenicity of breast cancer cells. *Cell* 131:1109–1123.

Zhang M, Dai C, Zhu H, Chen S, Wu Y, Li Q, Zeng X, Wang W, Zuo J, Zhou M, Xia Z, Ji G, Saiyin H, Qin L, Yu L. 2011. Cyclophilin A promotes human hepatocellular carcinoma cell metastasis via regulation of MMP3 and MMP9. *Mol Cell Biochem* 357:387–395.

SUPPORTING INFORMATION

Additional supporting information may be found in the online version of this article at the publisher's web-site.